Field Assessment of Alternative Bed-Load Transport Estimators

D. Gaeuman[1] and R. B. Jacobson[2]

Abstract: Measurement of near-bed sediment velocities with acoustic Doppler current profilers (ADCPs) is an emerging approach for quantifying bed-load sediment fluxes in rivers. Previous investigations of the technique have relied on conventional physical bed-load sampling to provide reference transport information with which to validate the ADCP measurements. However, physical samples are subject to substantial errors, especially under field conditions in which surrogate methods are most needed. Comparisons between ADCP bed velocity measurements with bed-load transport rates estimated from bed-form migration rates in the lower Missouri River show a strong correlation between the two surrogate measures over a wide range of mild to moderately intense sediment transporting conditions. The correlation between the ADCP measurements and physical bed-load samples is comparatively poor, suggesting that physical bed-load sampling is ineffective for ground-truthing alternative techniques in large sand-bed rivers. Bed velocities measured in this study became more variable with increasing bed-form wavelength at higher shear stresses. Under these conditions, bed-form dimensions greatly exceed the region of the bed ensonified by the ADCP, and the magnitude of the acoustic measurements depends on instrument location with respect to bed-form crests and troughs. Alternative algorithms for estimating bed-load transport from paired longitudinal profiles of bed topography were evaluated. An algorithm based on the routing of local erosion and deposition volumes that eliminates the need to identify individual bed forms was found to give results similar to those of more conventional dune-tracking methods. This method is particularly useful in cases where complex bed-form morphology makes delineation of individual bed forms difficult.

DOI: 10.1061/(ASCE)0733-9429(2007)133:12(1319)

CE Database subject headings: Bed load; Bedforms; Missouri River; Sediment transport; Assessments.

Introduction

The use of acoustic Doppler bottom-tracking technology to measure the velocity of near-bed sediment motion has emerged as an intriguing new approach to quantifying bed-load sediment fluxes in rivers. Although field comparisons (Rennie et al. 2002; Rennie and Villard 2004) have demonstrated positive correlations between acoustic Doppler bed velocity measurements (ν) and bed-load transport rates measured by conventional physical samplers, reliable and practical calibrations relating the acoustic measurements to actual transport rates have yet to be developed. Perhaps the greatest obstacle toward that end is a frustrating lack of reliable bed-load transport data against which acoustic techniques can be compared. The same may be said of other alternative approaches, such as tracking dune migration rates. Dune tracking is believed to have the potential to provide good estimates of bed-load transport rates in sand-bed systems under at least some flow conditions (Simons et al. 1965; Mohrig and Smith 1996; Villard and Church 2003). However, as with the newer acoustic methods, the practical development of dune tracking as a standard technique for estimating bed-load transport rates has been hampered by the lack of unequivocally correct transport measurements with which to validate the results.

In general, it is assumed that physical sampling is the most reliable method for determining the true bed-load transport rate. Although bed-load traps can be used in many small or coarse-bedded streams (Leopold and Emmett 1976; Laronne et al. 2003), sampling in large streams usually requires the use of one of several types of cable-suspended samplers (Edwards and Glysson 1999). It is well known that the quantities of sediment captured in bed-load samplers are highly variable in both space and time (Gray et al. 1991). To some extent, this variability may reflect real fluctuations in the transport process (Kleinhans and Ten Brinke 2001), but it seems clear that various types of sampling errors, such as dredging (Childers 1999), bed scour (Gaweesh and van Rijn 1994), and vacuuming effects (Pitlick 1988; Bunte et al. 2004), can significantly degrade sampling accuracy. Many of these difficulties are exacerbated when sampling in large sand-bed rivers where bed-load transport rates can be high, bed-form development is pronounced, and the placement of physical samplers on the bed is difficult to control or monitor. In such cases, there is arguably little basis to assume that physical samples more accurately represent the "true" bed-load transport rate than do the alternative techniques. In this paper, we compare three different methods for assessing the magnitude of bed-load transport: bed-load velocity measured with an acoustic Doppler current profiler (ADCP), bed-load transport rates computed from bed-form migration rates, and conventional bed-load sampling. Among our

[1]Geomorphologist, Trinity River Restoration Program, P.O. Box 1300, Weaverville, CA 59093 (corresponding author). E-mail: dgaeuman@usbr.gov

[2]Research Hydrologist, U.S. Geological Survey, Columbia Environmental Research Center, 4200 New Haven Rd., Columbia, MO 65201. E-mail: rjacobson@usgs.gov

Note. Discussion open until May 1, 2008. Separate discussions must be submitted for individual papers. To extend the closing date by one month, a written request must be filed with the ASCE Managing Editor. The manuscript for this paper was submitted for review and possible publication on April 5, 2006; approved on June 15, 2007. This paper is part of the ***Journal of Hydraulic Engineering***, Vol. 133, No. 12, December 1, 2007. ©ASCE, ISSN 0733-9429/2007/12-1319–1328/$25.00.

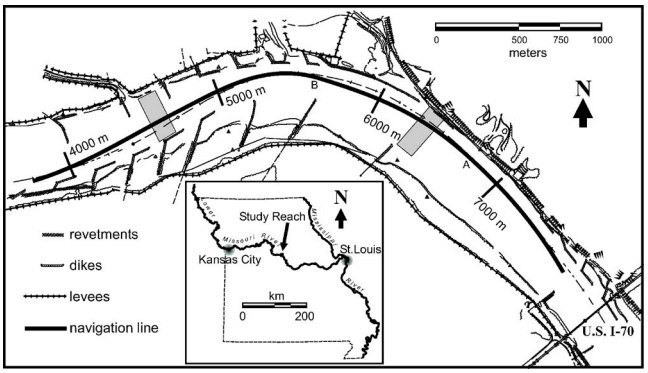

Fig. 1. Maps showing location and features of study reach. Flow direction is left to right. Shaded rectangles indicate locations of repeated bathymetric surveys, and locations labeled *A*, *B*, and *C* correspond to points depicted in Fig. 10.

basic premises is that spatial variability and the potential for large sampling errors associated with physical sampling are, under many field conditions, of a magnitude that renders the samples ineffective for ground-truthing the alternative techniques.

Study Reach

The present discussion is based on field data collected in a bend of the lower Missouri River located between about 0.5 and 5 km upstream from the U.S. Interstate 70 bridge in central Missouri (Fig. 1). The study reach begins just upstream from the crossing between a meander bend to the left and bend to the right, and continues through the length of the right-hand bend. This part of the Missouri River has been highly engineered, with continuously reverted banks and frequent wing dike structures designed to maintain a self-scouring navigation channel about 200 m in width. The bed of the navigation channel is composed primarily of sand with a median grain size of about 0.55 mm (Gaeuman and Jacobson 2006), and contains rapidly evolving bed forms. The morphology and dynamics of bed forms in the reach are described more fully below.

A U.S. Geological Survey stream flow gauging station (USGS 06909000, Missouri River at Boonville) is about 15 km upstream from the site. Thalweg depths range between about 7 and 10 m and depth-averaged flow velocities can exceed 3 m/s when the river is at flood stage at the Boonville gauge (about 4,670 m^3/s). Stream flows during the period of data collection fluctuated between relatively low flows maintained for navigation (1,100–1,200 m^3/s), and four brief rises that peaked at 4,048 m^3/s (May 15), 4,303 m^3/s (June 7), 5,464 m^3/s (June 14), and 2,831 m^3/s (October 5). More information regarding the hydrology during the study period is given in Gaeuman and Jacobson (2006).

Methods

Bed-Form Surveys

Dune morphology and migration data were obtained from longitudinal profiles of bed topography. We created a longitudinal navigation line that follows the approximate channel thalweg position through the study reach (Fig. 1). Precision depth-sounder and position data were recorded while steering our vessel along the navigation line with the aid of commercial navigation software and a real-time kinematic global positioning system (RTK-GPS) with positional accuracy of about 3 cm. Both the bathymetric and the positional data were logged at a rate of 5 Hz. Boat velocities were usually maintained near 3 m/s or less, resulting in a typical bathymetric sampling interval of about 0.6 m.

Dune migration rates were assessed using paired longitudinal profiles. Each day of data collection began by recording longitudinal profile data in a time-stamped digital file, each of which took about 20 min to complete. Following a period occupied by acoustic or physical bed-load sampling or related bathymetric surveying, a second profile was initiated anywhere between 1.5 and 2.5 h after the start time of the first profile. A total of 14 paired sets of profiles were collected on 14 different days between early April and early October, 2005.

Postprocessing of the raw bathymetric data included the projection of each individual sounding onto the navigation line with a custom computer script. In addition to bed elevation and distance downstream along the navigation line, output from the script included the distance and direction from the actual sounding location to its projected location on the navigation line. This made it possible to accurately determine the actual lateral distance between the first and second profiles at every location along the profile. In general, analyses of dune migration were performed where the actual boat paths for the first and second profiles coincided within about 1 m.

To assess bed-form organization in three dimensions, we also conducted repeated bathymetric surveys in two locations, each of which covered an area measuring 100 m in the streamwise direction and more than 200 m in the transverse direction. One of these areas is located in the crossing near the upstream end of the study reach, and the other a short distance downstream of the apex of the bend (Fig. 1). Surveys in both areas were conducted along planned navigation lines spaced 10 m apart and oriented perpendicular to the downstream flow direction. Bathymetry was obtained using a four-beam broadband 600 kHz Workhorse Rio Grande ADCP manufactured by RD Instruments, Inc., with integrated RTK GPS. Each of the instrument's four acoustic beams are oriented radially outward from vertical at an angle of 20°, so that topographic data were recorded from positions up to 0.34 (the tangent of the beam angle) times the flow depth on either side of the ship track. This allowed for the collection of more and more uniformly distributed bathymetric data than would be recorded using a single vertical beam. We developed a computer algorithm to compute the true geographic positions for soundings from each individual beam using the reported sounding depths, plus output from the ADCP's internal compass and tilt sensor. These data were subsequently gridded to 2-m resolution using commercial software to produce three-dimensional topographic surface models.

Acoustic Bed Velocity

Although research to determine the precise nature of the information contained in ADCP bed velocity measurements is ongoing, the general procedures by which the measurements are obtained are relatively straightforward. The basic requirements include the deployment of one of several commercially available acoustic Doppler profilers with bottom-tracking functionality. The instrument can be deployed in either a stationary position or from a mobile platform if high-quality global positioning system (GPS) is available to track instrument motion. Custom software utilities are used during postprocessing to extract bottom-track velocity

components from the logged data on a ping-by-ping basis, subtract any actual instrument velocity components if the platform is mobile, and output v data on a ping-by-ping or time-averaged basis. ADCP measurements reported here were obtained using the same vessel-mounted ADCP/GPS system used for bathymetric surveying. Details concerning the collection and processing of the ADCP data discussed in this paper can be found in Gaeuman and Jacobson (2006). Additional general information regarding field and data processing procedures necessary for measuring v, sources of error in those measurements, and design characteristics of specific instruments can be found in Rennie et al. (2002), Rennie and Villard (2004), and Gaeuman and Jacobson (2005).

Bed velocities intended for direct comparisons with dune-tracking results were recorded at various locations along the longitudinal profile navigation line during the time interval between the first and second runs of profile pairs. A total of 80 of these types of acoustic samples were obtained on 7 different days between June and October 2005. Discharges on the days these data were collected ranged from 1,090 to 5,465 m^3/s. An additional five acoustic samples collected prior to June were located near, but not directly over, the profile line, but are nonetheless included in the comparison between acoustic and morphology-based transport estimates. Samples consisted of several hundred individual pings obtained over sampling periods of at least 2 min to as much as 10 min while the boat was maintained in approximately the same location using engine power and GPS navigation. Minor longitudinal boat movements during sampling were used to obtain measurements that represent spatial averages over a larger region of the bed. Boat movements ranged from about 3 m to more than 10 m, resulting in an acoustic footprint on the bed spanning distances between about 10 and 16 m in both the longitudinal and transverse directions.

Among the possible error sources in these measurements is the potential for bottom-track velocities to be contaminated with backscatter from particles moving in the water column well above the bed. For example, Kostaschuk and Best (2005) noted that a 1,500 kHz instrument deployed in the Fraser River sometimes returned false bottom detections and unrealistically large bed-velocity measurements caused by high concentrations of suspended sediments in the water column. The strength of the signal backscattered from suspended particles depends on the particle sizes and the frequency of the instrument, with higher frequency instruments being more sensitive to the silt-sized particles that are likely to be concentrated in suspension. Because the instrument used to collect the Missouri River data reported here operates at 600 kHz, it is relatively insensitive to suspended particles. Gaeuman and Jacobson (2006) present a hydraulic analysis showing that bed velocities in the Missouri River data set are consistent with water velocities within a few cm of the bed surface. In addition, bathymetry obtained with the ADCP contained no anomalous depths indicating false bottom detections.

Physical Bed-Load Samples

Ninety four physical bed-load samples were collected in the navigation channel between late April and mid-June, 2005, using a BL-84 bed-load sampler with a 0.25 mm mesh bag. None of the bed-load samples reported on herein underwent laboratory sieve analysis, but they were superficially similar to 22 samples obtained in the same reach in 2004 that were sieved. The median grain sizes of the 2004 samples were found to range between 0.25 and 1.25 mm, with an average of 0.45 mm. Bed velocity measurements used for comparisons with physical bed-load samples were recorded simultaneously with sampler deployment. More information concerning the bed-load sampling and ADCP data collection procedures can be found in Gaeuman and Jacobson (2006). Although the acoustic sampling procedures used for comparisons with physical samples were similar to those obtained for dune-tracking comparisons, the two data sets were obtained at different times in different parts of the study reach. Thus, ADCP measurements are available for comparison with both physical bed-load samples and with dune-tracking results, but no physical samples are available for direct comparison with dune-tracking results.

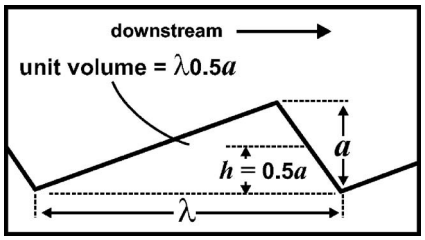

Fig. 2. Diagram indicating relationship between a, h, and β for triangular bed form with β=0.5

Bed-Load Transport from Dune Migration

Minimal requirements for estimating bed-load transport rates from bed-form migration include knowledge of bed-form dimensions and the bed-form migration velocity. A simple relation for computing the volumetric unit bed-load transport rate is (Simons et al. 1965)

$$q_b = 0.5(1-\varepsilon)a\frac{dx}{dt} + C_1 \tag{1}$$

where ε=porosity of the sediment composing the bed form; a=crest-to-trough amplitude of the bed form; and dx=downstream propagation distance of the bed form during time interval dt. The numerical coefficient of 0.5 implies that the bed forms under consideration are triangular in form when projected onto a vertical plane parallel to the downstream direction of migration (Fig. 2). Subsequent authors (Kostaschuk et al. 1989; Villard and Church 2003) replaced 0.5 with a coefficient, β, that accounts for deviations of bed-form shape from an idealized triangle. C_1 represents the portion of the bed-load flux that does not participate in the downstream translation of the bed form, as would be the case for particles that jump from one bed-form crest to the next bed-form downstream with no residence time on the intervening slip-face. Although Simons et al. (1965) point out that C_1 must scale from 0 at the threshold of particle entrainment to 100% of q_b under upper-regime plane-bed conditions, little is known concerning the magnitude of C_1 for the range of conditions in between. Field and laboratory experiments, as well as modeling results, suggest that C_1 may commonly account for more than half of q_b (Mohrig and Smith 1996). However, Simons et al. (1965) reported success in the laboratory using: (1) with $C_1=0$, and both Yang (1986) and Villard and Church (2003) reported that dune migration equations similar to Eq. (1) appeared to overpredict bed-load transport rates in their field studies, a result that also implies a small value for C_1. Some authors (Ten Brinke et al. 1999) prefer to incorporate C_1 into the shape factor β. The interpretation of C_1 is confounded to some extent by an inherent ambiguity regarding how bed load is distinguished from suspended

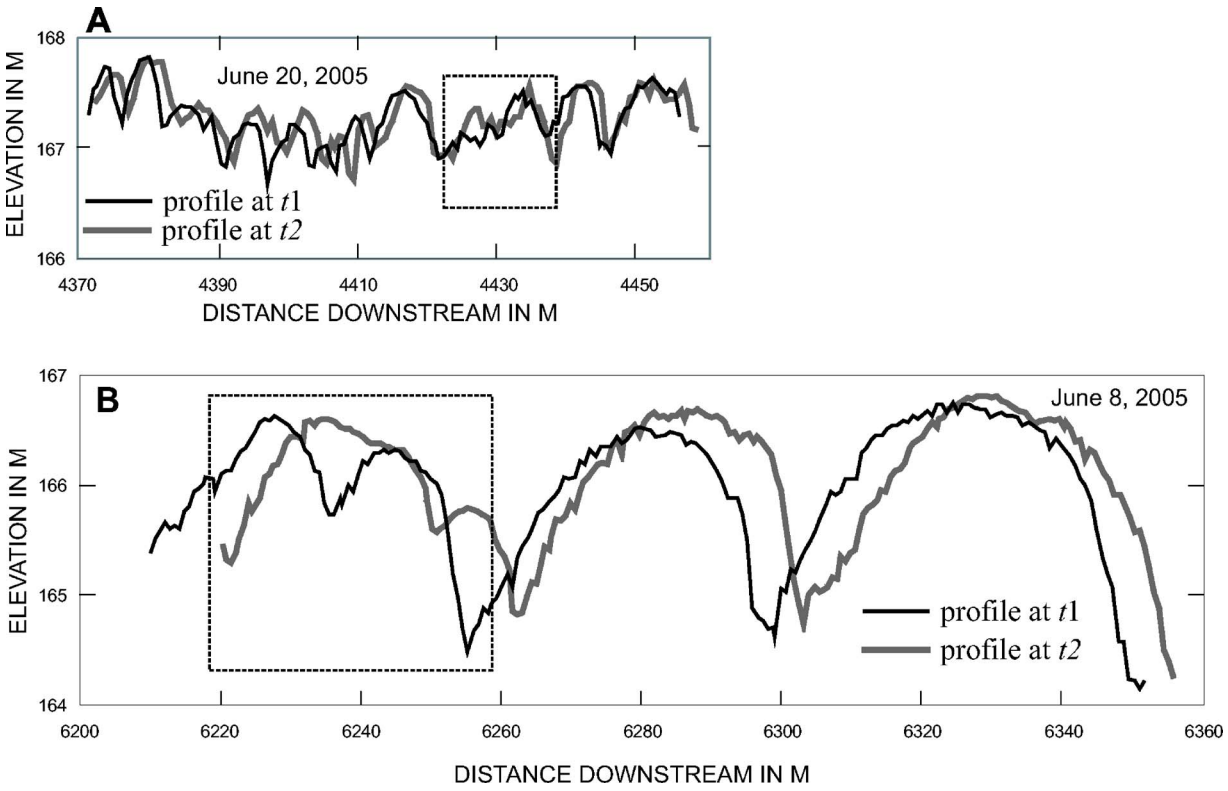

Fig. 3. Sections of paired bathymetric profiles along navigation line showing (A) small dunes; (B) large dunes. Both profile pairs are shown at same scale. Dashed boxes indicate (A) profile section where irregular morphology makes corresponding individual bed forms difficult to recognize; and (B) example of dunes appearing to merge in time interval between profiles.

bed-material load (Yang 1986; Villard and Church 2003). For present purposes, we define bed load as the portion of the bed-material load traveling close enough to the bed to be captured in a bed-load sampler, and simply recognize C_1 as an unknown and potentially significant term, such that equations similar to Eq. (1) are best regarded as a lower limit for the actual bed-load transport rate.

Another difficulty in evaluating Eq. (1) that can be as troublesome as determining C_1 is properly specifying bed-form dimensions. Bed forms can be highly variable in size and shape (Wewetzer and Duck 1999), and the presence of smaller bed forms superimposed on larger bed forms can make the identification of the relevant scale somewhat arbitrary [Fig. 3(a)]. These difficulties are exacerbated when analyzing bed-form migration, because individual bed forms can change shape, split in two, or merge together during the time interval over which migration is observed (Jerolmack and Mohrig 2005). Such morphologic distortions complicate the specification of bed-form dimensions and the identification of corresponding individual bed forms on successive profiles [Fig. 3(b)].

In recognition of the foregoing uncertainties we applied and compared three separate procedures for calculating bed-load transport rates from paired bed-form profiles. It is useful at this point
to introduce notation that clearly identifies the bed-form features under consideration. Soundings in any local area of the first longitudinal profile in a profile pair were recorded at time $t1$. Sounding in the same local area of the second profile of the pair were recorded at time $t2$, where $t2=t1+dt$. To estimate the bed-load transport rate in any local area, it is necessary to consider the dimensions and migration rates of one or more dunes that can be recognized as the same feature on both profiles. These individual dunes can be designate as $d_{n,t}$, where $n=1\ldots N$, N is the number of dunes included in the local analysis, and t can be $t1$ or $t2$.

We first computed bed-load transport rates using a straightforward implementation of Eq. (1) with C_1 assumed equal to zero and the coefficient of 0.5 replaced with 0.6 as suggested by Villard and Church (2003). This method, which we designate as Method 1, requires the visual inspection of paired sounding traces to manually identify the individuals corresponding to $d_{n,t}$ for all N in each local area where a bed-load transport estimate is desired. For each n and t the positions of the leading and trailing troughs ($tl_{n,t}$ and $tt_{n,t}$, respectively) and the dune peaks ($p_{n,t}$) are manually recorded. Although this identification requires a certain degree of subjective judgment, in most cases it was possible to define the primary peaks and troughs with reasonable confidence. Bed-load computations were not attempted in cases where erratic dune morphology made correlation across profile pairs ambiguous. The amplitudes of individual dunes were computed at times $t1$ and $t2$ as the differences between the peak elevations and the average elevations of the leading and trailing troughs, $a_{n,t}=p_{n,t}-(tl_{n,t}+tt_{n,t})/2$. The mean amplitude for dune n was then determined as the arithmetic average over time for each dune: $a_n=[a_{n,t1}+a_{n,t2}]/2$. We chose to compute the mean positions of individual dunes at time t ($x_{n,t}$) as the average of the downstream distances measured along the profile line to its leading trough, its trailing trough, and its peak. The migration distance input to Eq. (1) for dune n is $dx_n=x_{n,t2}-x_{n,t1}$. The local bed-load transport rate for a sequence of N dunes is computed as the average of the individual transport rates determined according to Eq. (1), where each transport rate is weighted by the fraction of the total se-

quence length occupied by wavelength n. As Method 1 is especially labor intensive, it was used primarily to check for errors in the implementation of Method 2, described below.

Method 2 constitutes an improvement over Method 1 in terms of both efficiency and accuracy. Rather than estimating bed-form volume on the basis of maximum height and an assumed shape factor, Method 2 computes volume directly from the profiles. A computer algorithm was developed to define a datum representing the base of the mobile part of the bed by connecting successive bed-form troughs on each profile with a straight line. The algorithm then numerically integrates the area between the datum and the bed-form surface, and division by length yields a mean height for each bed form, $h_{n,t}$. The time average of these mean heights is computed by $h_n=(h_{n,t1}+h_{n,t2})/2$ for use in a modified version of Eq. (1) in which no shape parameter is required

$$q_b = (1-\varepsilon)h\frac{dx}{dt} \tag{2}$$

As a by-product of integrating the area under the bed-form curve, it is convenient to compute the shape factor β and the downstream position of each dune's center of mass, $m_{n,t}$. The latter parameter was used in the computation of the mean position of each dune as the arithmetic average of $m_{n,t}$ and the midpoint between its leading and trailing troughs: $x_{n,t}=0.5(m_{n,t}+[tl_{n,t}+L/2])$, where $L=tt_{n,t}-tl_{n,t}$. As in Method 1, $dx_n=x_{n,t2}-x_{n,t1}$ and the transport rate for the entire bed-form sequence is determined as the weighted average of the transport rates determined for individual dunes.

Method 3 was developed to eliminate the need to identify and correlate each individual dune in a local analysis. Instead, Method 3 requires only the specification of the x positions of the most upstream and the most downstream troughs in a section of paired profiles of arbitrary length. The position of the upstream trough is defined at time $t1$, and the position of the downstream trough is defined at time $t2$. A major advantage of Method 3 is that it can be applied to regions of the bed where some of the bed forms within a sequence of forms cannot be reliably correlated across profiles. The method implements a budgeting approach in which the local volumetric bed-load flux per unit bed width at any point along the profile is related to upstream volumes of erosion and downstream volumes of deposition. As a first step, it is necessary to resample the projected soundings in each profile to a small, regularly spaced dx (0.1 m). The downstream positions and elevations between actual soundings are interpolated, so the resampling procedure results in virtually no information loss and a substantial improvement in the precision of numerical integration. At each point along the resampled profile pair, the bed elevation at time $t2$ ($z_{x,t2}$) is subtracted from the bed elevation at time $t1$ ($z_{x,t1}$) to yield dz_x. Erosion is recorded where dz_x is positive, and deposition is recorded where dz_x is negative. Locations where dz_x changes sign are designated as the beginning and end nodes of local regions of either erosion or deposition, resulting in the definition of an alternating sequence of N deposition regions and N erosion regions (Fig. 4). Straight lines connecting the points of minimum elevation between adjacent nodes define the base of the active bed layer that is scoured and filled in association with the passing of a bed-form trough. These base lines are combined with boundaries corresponding to the minimum of $z_{x,t1}$ or $z_{x,t2}$ to form $N-1$ closed, approximately triangular regions where both erosion and deposition occurred during the interval dt. Each of these regions is appended to both the deposition region immediately upstream and the erosion region immediately downstream, such that the deposition and erosion regions acquire a spatial overlap.

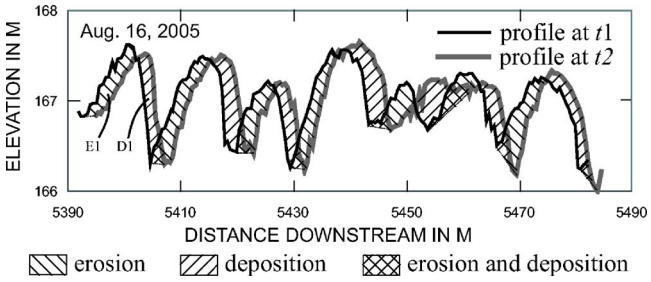

Fig. 4. Section of paired bathymetric profile illustrating erosion and deposition regions defined for Method 3 dune tracking analysis. Ideally, sediment continuity requires that $E1=D1$ with maximum bed-load fluxes occurring at intersection of $E1$ and $D1$ near the bed-forms crest. Bed forms shown average about 15 m in wavelength, putting them near upper limit of size range for small dunes.

Erosion regions tend to encompass the upper stoss faces and crests of bed forms, as depicted at time $t1$, whereas deposition regions tend to encompass the slip faces and trough portions of the $t1$ forms. As the entire unit volume of sediment mobilized from an erosion region must pass the node linking the erosion region to a downstream deposition region, the volume of sediment passing these points represents local maxima. This can be written symbolically as $V(x_0)=E$, where $V(x_0)=$sediment volume passing point x_0; $x_0=$location of the transition from erosion to deposition; and $E=$total erosion volume from the upstream erosion region. For a point x located dx upstream from x_0, the sediment passing x is decreased by the volume of the local erosion source area located downstream from x, or $V(x)=E-dz_x dx$. Moving another step upstream to $x-dx$, $V(x-dx)=E-(dz_x dx+dz_{x-dx}dx)$, and so on. Likewise, it can be assumed that the volume of sediment passing x_0 is equal to the total volume deposited in the deposition region immediately downstream, or $V(x_0)=D$. For x located dx downstream from x_0, $V(x)=D-|dz_x dx|$, $V(x+dx)=E-|dz_x dx+dz_{x-dx}dx|$, and so forth. In areas where upstream deposition regions overlap with downstream erosion regions, the incremental flux at each x is computed as the sum of the deposition volume remaining downstream from the point and the portion of the erosion region lying upstream from the point. The mean volumetric flux rate for the portion of the profile pair being analyzed is computed as the arithmetic average of all the incremental fluxes, divided by dt.

The scheme described above implicitly assumes that each E is equal in unit volume to the D located immediately downstream. This equality cannot be expected in practice. Any number of factors could result in a lack of perfect mass continuity across a bed-form crest, including lateral sediment transport, imperfect depth-sounder precision, finite sampling density, or spatial variability in C_1 at the local scale. For a profile sequence consisting of multiple individual bed forms, spatial averaging of the incremental fluxes should minimize the effect of random measurement errors on the final transport estimate. Preliminary examination of the spatial distribution of fluxes at the incremental scale (that is, at each dx) has revealed occasional disparities in the flux rates computed from upstream erosion regions and downstream deposition regions at region interfaces, but these imbalances in sediment continuity do not appear to be pervasive or systematic in nature. Where present, the discontinuities may indicate actual changes in the sediment transport process.

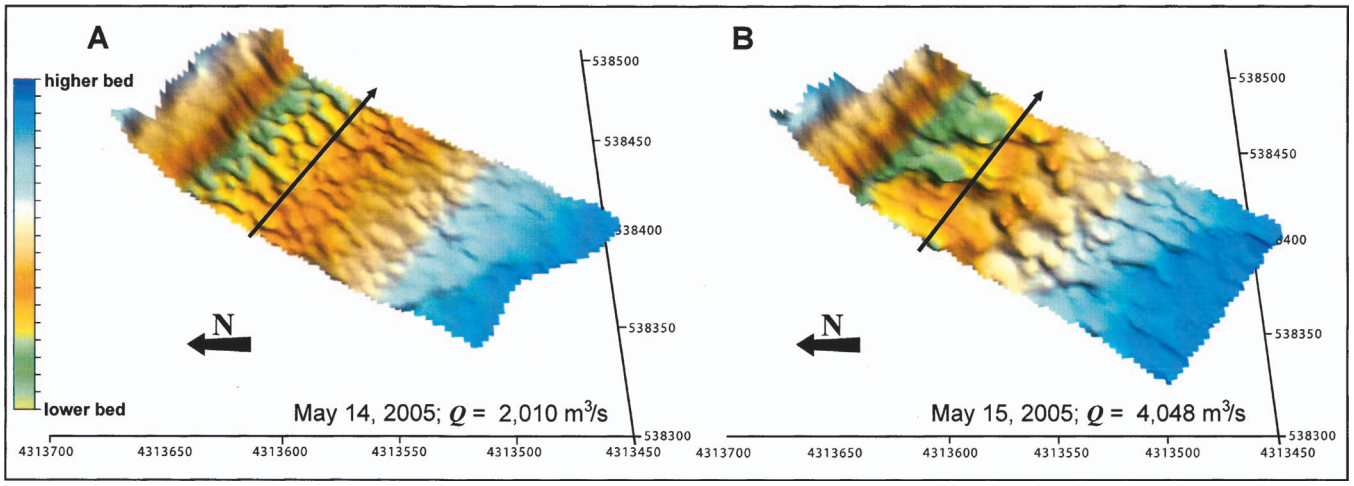

Fig. 5. (Color) Mesoscale maps of bed bathymetry in more downstream of two shaded areas shown in Fig. 1. Flow direction and path of profile navigation line are indicated by thin arrows superimposed on maps. Small dunes in thalweg developed into large dunes within approximately 24 h during rising stage between May 14 and May 15.

Methods 2 and 3 were used to estimate local bed-load transport rates corresponding to ADCP samples collected at known positions along the profile navigation line. The length of the local profile sequences and the number of bed forms incorporated into each estimate varied according to bed-form wavelengths and the local availability of identifiable forms. Use of a larger N in a sequence necessarily requires the use of bed forms located farther from the location where ADCP data were recorded, particularly when bed-form wavelengths are large. It was sometimes necessary to restrict sequence length or exclude portions of sequences near the point of ADCP measurement because erratic bed morphology interfered with bed-form delineation. In general, profile sequences used to estimate local bed-load transport rates were 50–150 m in length, and consisted of between three and nine individual dunes. All transport estimates were computed using a nominal value of $\varepsilon=0.3$ and converted to mass transport rates using an assumed mineral density of 2,650 kg/m^3. To distinguish them from volumetric transport rates computed for individual dunes, mass bed-load transport rates estimated for sequences of dunes are hereafter denoted g_b (kg s^{-1} m^{-1}).

Results and Discussion

Bed-Form Characteristics

Bed-form morphology varies with location in the study reach and with discharge. We recognize two end-member types of bed forms in the study reach, which we refer to simply as small dunes and large dunes. Small dunes range from less than 10 m to around 15 m in wavelength, and from about 0.5 to 1.5 m in amplitude [Figs. 3(a) and 4]. Large dunes range between about 30 and 60 m in wavelength and are frequently 2 m or more in amplitude [Fig. 3(b)]. Aside from their greater size, large dunes are distinguished from small dunes in that they tend to develop broad rounded crests and narrow troughs. Similar rounded dune forms have been reported in the Fraser River (Kostaschuk and Villard 1996). Both types of bed forms are oriented with their crests approximately perpendicular to the downstream flow direction and the navigation line used to survey bathymetric profiles (Fig. 5). Thus, the surveyed profiles provide good approximations of actual bed-form dimensions and downstream migration rates.

Small dunes are widespread in the navigation channel during periods of low discharge, whereas large dunes are generally restricted to a section of the thalweg downstream from the bend apex. With increasing discharge, the portion of the thalweg occupied by large dunes expands upstream and downstream. Bed-form response to changing flow conditions is rapid, particularly during periods of rising stage (Fig. 5). As discharge approaches flood stage, small dunes become increasingly restricted to the crossing area and channel margins.

Dune Tracking and Bed Velocity

A comparison of 40 estimates of g_b obtained from Methods 1 and 2 confirmed that the two techniques give similar results. Minor differences between the two methods can be attributed to differences between the assumed value of $\beta=0.6$ used in Method 1 and the actual values computed by the Method 2 algorithm. The average computed value for β of 0.58 (standard deviation=0.05) is typical of values reported elsewhere; for example Ten Brinke et al. (1999) found $\beta=0.55$ and Venditti et al. (2005) found $\beta=0.56$. Dune migration rates determined by either method are predominantly between about 1 and 5 m/h, with an average of 2.6 m/h. Migration rate scales weakly with dune height and wavelength, but inversely with dune steepness (Fig. 6). Steepness is defined as the crest-to-trough amplitude divided by wavelength.

Methods 2 and 3 also produced similar estimates of g_b, with substantial discrepancies occurring for just 3 of 85 data pairs (Fig. 7). These cases of disagreement correspond to profile segments where bed-form morphology is complex and bed-form delineation errors are likely. As Method 3 does not require the identification of individual bed forms, it is assumed to be more nearly correct in these cases. Thus, of the three dune-tracking methods considered in this paper, Method 3 appears to be superior in terms of both convenience and accuracy.

Given the data available in this study, two approaches are available for assessing the absolute accuracy of g_b calculated from dune tracking: comparison with the corresponding v measurements or an analytical approach based on measured hydraulic parameters. The correspondence between g_b determined from Method 3 dune tracking and v recorded at corresponding points

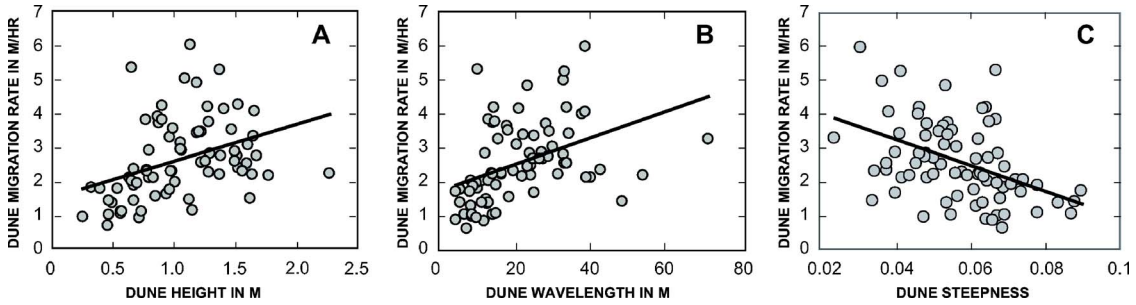

Fig. 6. Graphs of dune migration rate as function of: (A) dune height; (B) dune wavelength; and (C) dune steepness

along the bed-form profile line is reasonably strong, especially for g_b less than about 0.9 kg s^{-1} m^{-1} (Fig. 8). The geomorphic significance of this unit transport rate can be evaluated by casting it in terms of an annual load. Assuming an active bed width of 200 m, 0.9 kg s^{-1} m^{-1} is equivalent to an annual bed-load flux of 6.3 million t, or about 8% of the total annual Missouri River suspended sediment load delivered to the Mississippi River (Keown et al. 1986). As bed load is typically less than 10% of the suspended load in larger rivers (Inman and Jenkins 1999), the range of conditions over which dune-tracking results are in good agreement with ν extends to moderately high, geomorphically effective transport rates.

An alert reader may note that many of the values of ν indicated in Fig. 8 are quite large compared to values reported elsewhere (e.g., Rennie et al. 2002; Rennie and Villard 2004). Gaeuman and Rennie (2006) compared data from Sea Reach of the Fraser River with data from the Missouri River and reported that the maximum ν obtained in Sea Reach was 0.18 m/s, whereas the maximum ν obtained in the Missouri River was 0.62 m/s. However, flow velocities, shear stresses, and sediment transport rates were all found to be considerably larger in the Missouri River as well, as are the bed-form migration rates reported herein. Villard and Church (2003) reported that bed-form migration rates in the Fraser River estuary range between about 0.03 and 0.9 m/h, whereas migration rates in the Missouri River are an order of magnitude larger (Fig. 6). When differences in particle sizes, shear stresses, and instrument frequencies are considered, the difference between the values of ν observed in the two rivers is consistent with the physical principles governing acoustic response (Gaeuman and Rennie 2006).

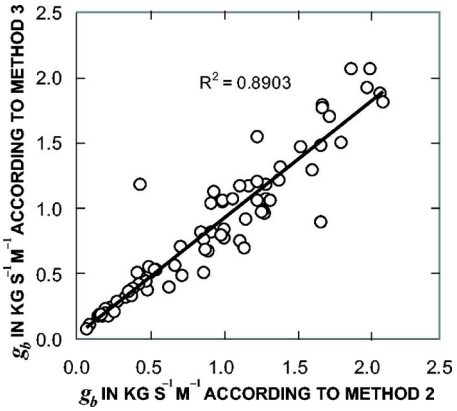

Fig. 7. Graph of relationship between bed-load transport rates estimated by dune-tracking Methods 2 and 3

Gaeuman and Jacobson (2006) have previously reported a positive correlation between ν measured in the Missouri River and flow strength, as expressed in terms of transport stage

$$T^* = \tau_{sk}/\tau_c \tag{3}$$

where τ_c=critical shears stress, assumed equal to 0.04 (Wilcock 1998), and τ_{sk}=shear stress related to grain resistance, which we estimated using the method proposed by Van Rijn (1984a). The relationship was observed to be especially strong for T^* less than about 17. However, the scatter in the relationship increased markedly for large T^*. Gaeuman and Jacobson (2006) suggested that increased variability in ν at higher transport stages is related to changes in bed-form morphology at higher stages, and associated changes in the spatial distribution of bed-load transport. However, an attempt to model the effect was only partially successful. Regardless of its cause, increased variability in ν at high T^* is responsible for the increase in scatter for $g_b > 0.9$ kg s^{-1} m^{-1}. Plotting g_b against T^* shows that g_b=0.9 kg s^{-1} m^{-1} corresponds to T^* near 17, the value associated with increased variability in ν (Fig. 9).

Given that g_b estimated from dune tracking represents a spatial and temporal average at scales on the order of 10^2 m and 10^3 s, whereas ν is measured at scales of 10–20 m and 10^2 s, it could be argued that the correspondence between ν and g_b shown in Fig. 8 is remarkably good. Indeed, consideration of individual measurements suggests that much of the variability at higher transport rates can be traced to scale effects. As noted above, increasing

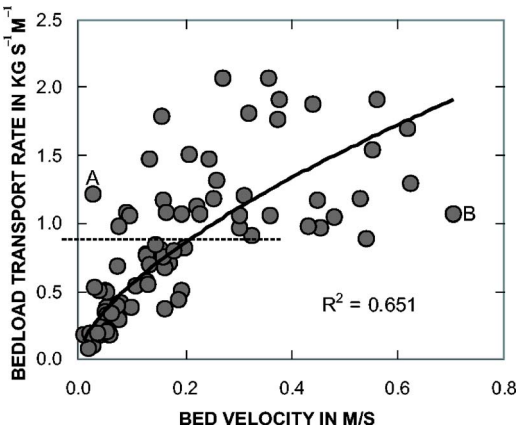

Fig. 8. Graph showing relationship between bed-load transport rates estimated from dune-tracking Method 3 and ADCP bed velocities. Correlation is particularly strong for $g_b < 0.9$ kg/s^{-1} m^{-1}, as indicated by dashed line. Bathymetry associated with anomalously high and low values of ν labeled A and B is depicted in Fig. 10.

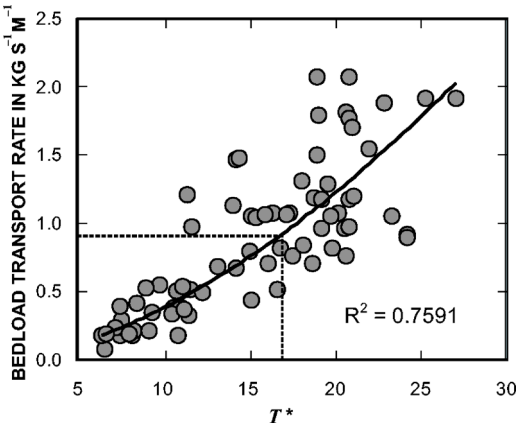

Fig. 9. Graph showing bed-load transport rates estimated from dune-tracking Method 3 as function of transport stage. Dashed lines show that $g_b < 0.9$ kg/s^{-1} m^{-1} corresponds to transport stage of about 17. Plotted curve fits data somewhat better than straight line, but no physical implications are intended.

discharge and sediment transport in the study reach are associated with a shift from small to larger dunes. Small dunes are typically 15 m in wavelength or less, and the ADCP measurements typically span a similar longitudinal extent of the bed. Measurements of ν at lower flows are therefore averaged over most or all of a full wavelength, as are the transport estimates obtained from dune tracking. However, the wavelengths of larger bed forms exceed the longitudinal extents of the ADCP measurements, sometimes by a factor of five or more. In these cases, ν reflects local transport rates over relatively small portions of the bed form. Inspection of individual measurements indicates that anomalously low ν values are recorded if the ADCP happens to be positioned over the trough of a relatively large bed form, whereas especially high ν values are associated with instrument positions over crests (Fig. 10).

Greater variability in ν at high T^* is reflected in the occurrence of much larger maximum values of ν for small values of dune steepness (Fig. 11). Larger ν can evidently evolve over relatively broad, flat regions of the bed, which are more available at higher excess shear stresses. Although both dune wavelength and dune height were observed to increase with excess shear stress, wavelength increases at a greater rate so that steepness decreases at

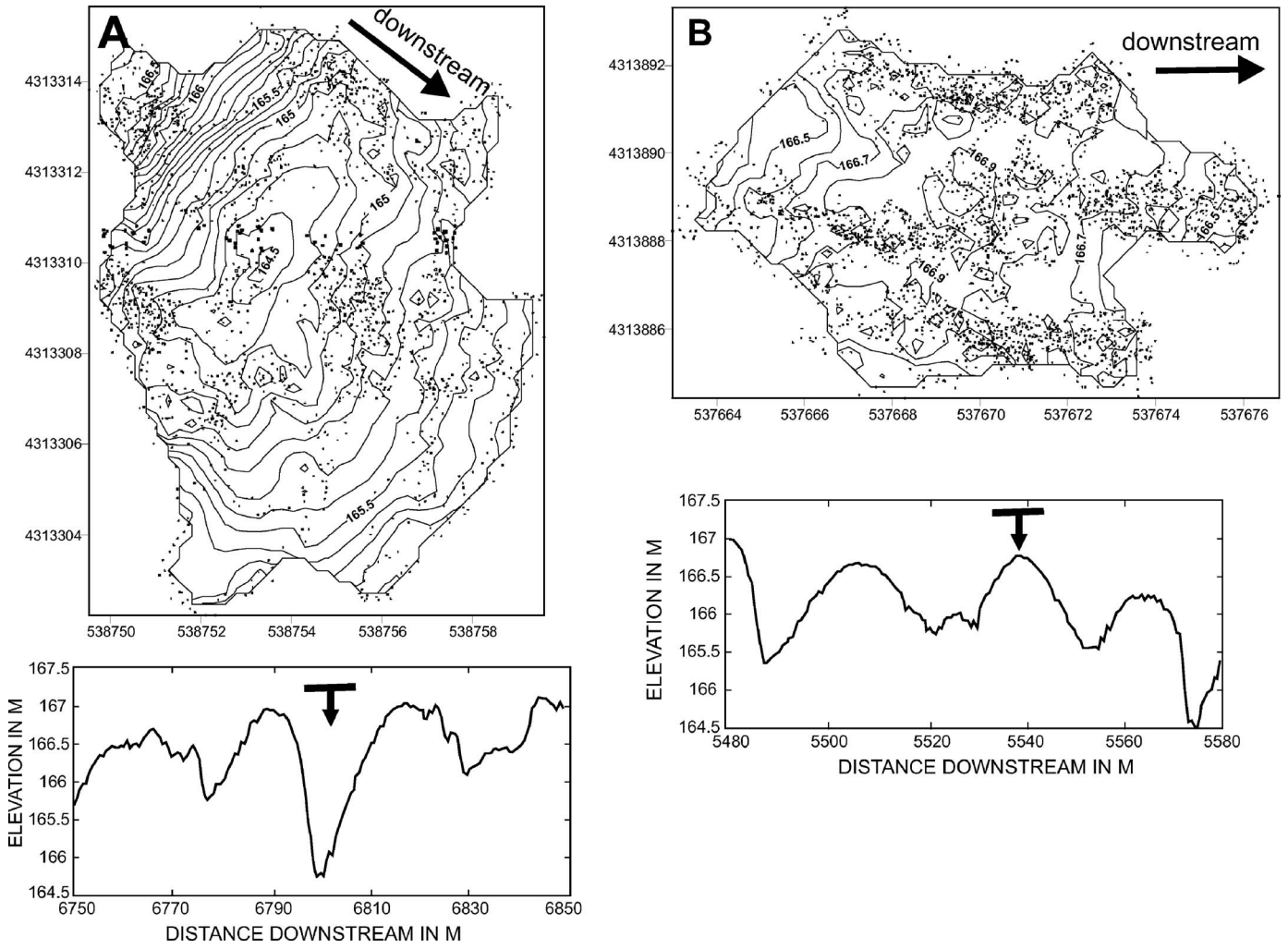

Fig. 10. Local bed topography in areas ensonified by ADCP beams in two example locations corresponding to anomalously high and low ν labeled in Fig. 8. Contour maps were created by gridding bed elevations recorded independently by each acoustic ping from each of four acoustic beams (small black dots) to 0.25-m resolution. Downward-pointing arrows with horizontal lines on profiles below each map indicate downstream positions and approximate longitudinal extents of ensonified areas.

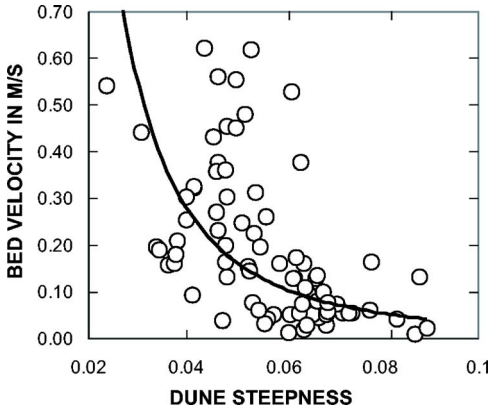

Fig. 11. Graph of bed velocity as function of dune steepness. High bed velocities are associated with flatter dunes.

high T^*. Similar decreases in dune steepness at higher transport stages have been reported by numerous previous investigators (Yalin and Karahan 1979; Van Rijn 1984b; Karim 1995).

Physical Sampling and Bed Velocity

By comparison, the correlation between v recorded in conjunction with physical bed-load sampling is poor over the range of flow and sediment transport conditions observed in the navigation channel (Fig. 12). If the physical samples are assumed to accurately represent the true bed-load transport rate, v must be regarded as a rather ineffective estimator. By virtue of the correspondence between v and the dune-tracking results, at least for the range $T^* < 17$ if not for all T^*, dune tracking must be regarded as ineffective as well. Such a position would be difficult to defend, since it would seem to imply that the relationship shown in Fig. 8 is coincidental. Instead, these data strongly suggest that both dune tracking and v offer a more consistent and reliable means for estimating bed-load transport rates than does physical sampling under the field conditions encountered in this study.

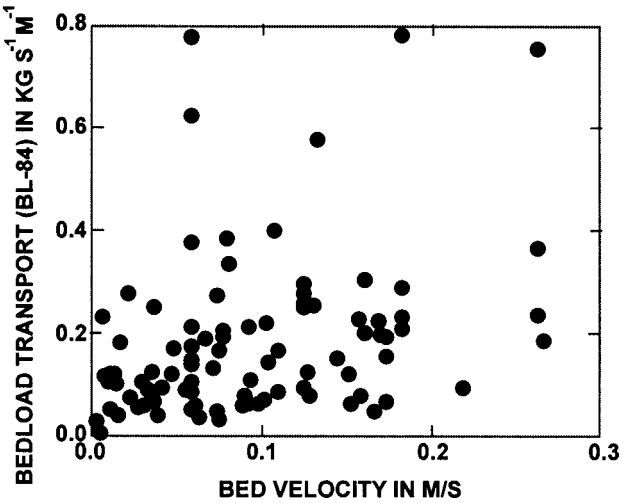

Fig. 12. Graph showing poor relationship between bed-load transport rates based on paired physical samples and ADCP bed velocities obtained in navigation channel

Conclusions

Bed-load transport rates estimated from dune migration rates correlate well with bed velocity measurements over a wide range of mild to moderately intense sediment transporting conditions in the lower Missouri River. Bed velocities become more variable and increase more quickly than transport estimates from dune tracking as skin friction exceeds about 17 times the threshold for particle entrainment ($T^* > 17$). Increased variability in the acoustic measurements under these flow conditions likely reflects the increased spatial scale of the bed-load transport field as dune wavelengths increase. Dune wavelengths were frequently five or more times greater at higher shears stresses, whereas the area of bed sampled with the ADCP remained relatively constant. The relatively slow rate of increase in the bed-load transport rates estimated from dune tracking at higher excess shear stresses suggests that the quantity of bed material that bypasses bed forms without contributing to the downstream migration of the form increases rapidly for $T^* > 17$.

Relative to the correspondence between bed velocity and dune tracking, the relation between bed velocities and physical bed-load samples obtained in the same reach is poor. Of these three approaches, conventional physical sampling appears to be the least reliable means for estimating bed-load transport rates in large sand-bed rivers. Thus, physical sampling cannot be considered an effective mean for evaluating the performance of the alternative measurements.

Standard methods for estimating bed-load transport rates from bed-form migration require the identification and correlation of individual bed forms at two or more points in time, and a means for estimating the volumes of individual bed forms. These volume estimates are sometimes obtained as the maximum bed-form height multiplied by a shape factor, which is frequently assumed to be equal to about 0.6. More accurate results can be obtained by calculating bed-form volumes numerically, thus eliminating the need for a shape factor. In addition, we developed and tested a new method for estimating bed-load transport rates from dune migration that eliminates the need to identify individual bed forms. The method computes local sediment fluxes over a contiguous series of bed forms of arbitrary length on the basis of local erosion and deposition volumes and the principle of mass continuity. The resulting transport estimates generally agreed with those derived from analyses based on individual bed-form identification. However, the new method is easier to implement, and produces better results in cases where bed-form morphology is complex or significant temporal distortion occurs.

References

Bunte, K., Abt, S. R., Potyondy, J. P., and Ryan, S. E. (2004). "Measurement of coarse gravel and cobble transport using portable bedload traps." *J. Hydraul. Eng.*, 130(9), 879–893.

Childers, D. (1999). "Field comparisons of six pressure-difference bed-load samplers in high-energy flow." *U.S. Geological Survey, Water Resources Investigations Rep. No. 92-4068*.

Edwards, T. E., and Glysson, G. D. (1999). "Field methods for measurement of fluvial sediment." *U.S. Geological Survey, Techniques of Water Resources Investigations 3-C2*.

Gaeuman, D., and Jacobson, R. B. (2005). "Aquatic habitat mapping with an acoustic Doppler current profiler: Considerations for data quality." *U.S. Geological Survey, Open File Rep. No. 2005-1163*.

Gaeuman, D., and Jacobson, R. B. (2006). "Acoustic bed velocity and bedload dynamics in a large sand-bed river." *J. Geophys. Res.*, 111,

F02005.
Gaeuman, D., and Rennie, C. D. (2006). "A comparison of two field investigations into acoustic bed velocity: General responses and instrument frequency effects." *Proc., 8th Federal Interagency Sedimentation Conf.*, Reno, Nev.
Gaweesh, M. T. K., and van Rijn, L. C. (1994). "Bedload sampling in sand-bed rivers." *J. Hydraul. Eng.*, 120(12), 1364–1384.
Gray, J. R., Webb, R. H., and Hyndmann, D. W. (1991). "Low-flow sediment transport in the Colorado River." *Proc., 5th Federal Interagency Sedimentation Conf.*, S.-S. Fan and Y.-H. Kuo, eds., U.S. Subcommittee on Sedimentation, 4, 63–71.
Inman, D. L., and Jenkins, S. A. (1999). "Climate change and the episodicity of sediment flux of small California rivers." *J. Geol.*, 107, 251–270.
Jerolmack, D., and Mohrig, D. (2005). "Interactions between bed forms: Topography, turbulence, and transport." *J. Geophys. Res.*, 110, F02014.
Karim, F. (1995). "Bed configuration and hydraulic resistance in alluvial-channel flows." *J. Hydraul. Eng.*, 121(1), 15–25.
Keown, M. P., Dardeau, Jr., E. A., and Causey, E. M. (1986). "Historic trends in the sediment flow regime of the Mississippi River." *Water Resour. Res.*, 22(11), 1555–1564.
Kleinhans, M. G., and Ten Brinke, W. B. M. (2001). "Accuracy of cross-channel sampled sediment transport in large sand-gravel-bed rivers." *J. Hydraul. Eng.*, 127(4), 258–269.
Kostaschuk, R., and Best, J. (2005). "Response of sand dunes to variations in tidal flow: Fraser Estuary, Canada." *J. Geophys. Res.*, 110, F04S04.
Kostaschuk, R. A., Church, M. A., and Luternauer, J. L. (1989). "Bed-material, bedforms and bed load in a salt-wedge estuary—Fraser River, British Columbia." *Can. J. Earth Sci.*, 26, 1440–1452.
Kostaschuk, R., and Villard, P. (1996). "Flow and sediment transport over large subaqueous dunes: Fraser River, Canada." *Sedimentology*, 43, 849–863.
Laronne, J. B., Alexandrov, J., Bergman, N., Cohen, H., Garcia, C., Habersack, H., Powell, D. M., and Reid, I. (2003). "The continuous monitoring of bedload flux in various fluvial environments." *Erosion and sediment transport measurement in rivers: Technological and methodological advances*, J. Bogen, T. Fergus, and D. E. Walling, eds., International Association of Hydrological Sciences, Publication 283, Wallingford, U.K., 134–145.
Leopold, L. B., and Emmett, W. W. (1976). "Bedload measurements, East Fork River, Wyoming." *Proc. Natl. Acad. Sci. U.S.A.*, 73(4), 1000–1004.
Mohrig, D., and Smith, J. D. (1996). "Predicting the migration of dunes." *Water Resour. Res.*, 32(10), 3207–3217.
Pitlick, J. (1988). "Variability of bed load measurement." *Water Resour. Res.*, 24(1), 173–177.
Rennie, C. D., Millar, R. G., and Church, M. A. (2002). "Measurement of bed load velocity using an acoustic Doppler current profiler." *J. Hydraul. Eng.*, 128(5), 473–483.
Rennie, C. D., and Villard, P. V. (2004). "Site specificity of bedload measurement using an acoustic Doppler current profiler." *J. Geophys. Res.*, 109, F03003.
Simons, D. B., Richardson, E. V., and Nordin, C. F., Jr. (1965). "Bedload equations for ripples and dunes." *U.S. Geol. Surv. Prof. Pap.*, 462-H.
Ten Brinke, W. B. M., Wilbers, A. W. E., and Wesseling, C. (1999). "Dune growth, decay and migration rates during a large-magnitude flood at a sand and mixed sand-gravel bed in the Dutch Rhine River system." *Fluvial sedimentology VI*, N. D. Smith and J. Rogers, eds., Blackwell Science, Oxford, U.K., 15–32.
Van Rijn, L. C. (1984a). "Sediment transport. I: Bed load transport." *J. Hydraul. Eng.*, 110(10), 1431–1456.
Van Rijn, L. C. (1984b). "Sediment transport. III: Bed forms and alluvial roughness." *J. Hydraul. Eng.*, 110(12), 1733–1754.
Venditti, G., Church, M., and Bennett, S. J. (2005). "Morphodynamics of small-scale superimposed sand waves over migrating dune bed forms." *Water Resour. Res.*, 41, W10423.
Villard, P. V., and Church, M. (2003). "Dunes and associated sand transport in a tidally influenced sand-bed channel: Fraser River, British Columbia." *Can. J. Earth Sci.*, 40, 115–130.
Wewetzer, S. F. K., and Duck, R. W. (1999). "Bedforms in the middle reaches of the Tay Estuary, Scotland." *Fluvial sedimentology VI*, N. D. Smith and J. Rogers, eds., Blackwell Science, Oxford, U.K., 33–41.
Wilcock, P. R. (1998). "Two-fraction model of initial sediment motion in gravel-bed rivers." *Science*, 280, 410–412.
Yalin, M. S., and Karahan, E. (1979). "Steepness of sedimentary dunes." *J. Hydr. Div.*, 105(4), 381–392.
Yang, C.-S. (1986). "On Bagnold's sediment transport equation in tidal marine environments and the practical definition of bedload." *Sedimentology*, 33, 465–486.